

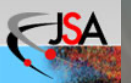
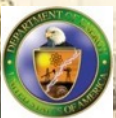
Exclusive physics at JLAB: Overview

S. Stepanyan

Jefferson Lab

HEP2023, Jan. 9-13, 2023

UTFSM, Valparaíso, Chile

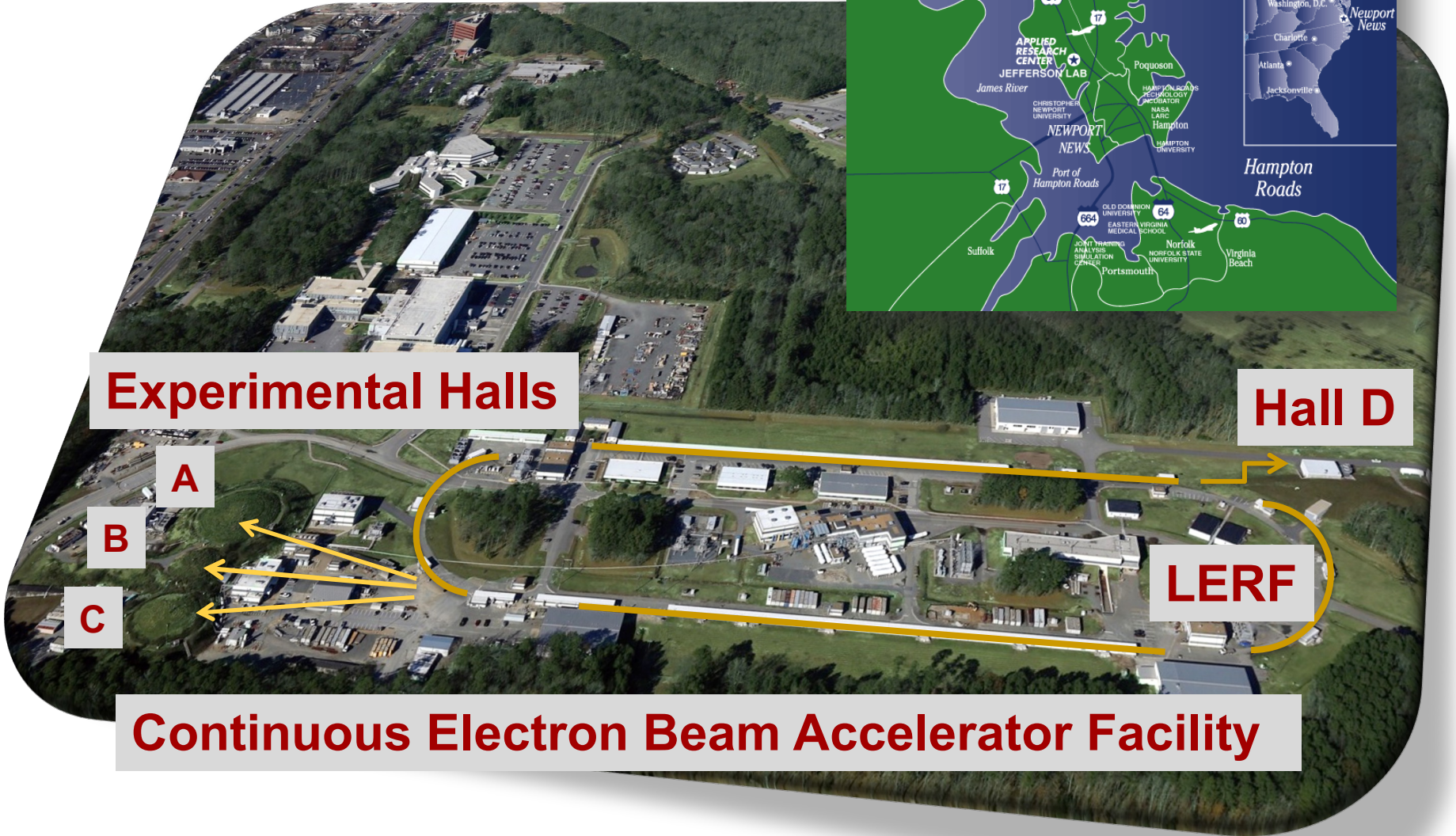


Outline

- Jefferson Lab CEBAF and experimental apparatus
- Overview of physics program
- Elastic scattering and EM FFs
- Exclusive processes and GPDs
 - Deeply Virtual Compton Scattering (DVCS)
 - Time-like Compton Scattering (TCS)
 - Deep Virtual Meson production (DVMP)
 - Near threshold J/ψ production
- Future opportunities
- Summary



Jefferson Lab



Experimental Halls

Hall D

LERF

Continuous Electron Beam Accelerator Facility



S. Stepanyan, HEP2023, Jan. 9-13,
UTFSM, Valparaíso, Chile



Experimental Setups



Hall-A: SBS & BB



Hall-B: CLAS12



Hall-C: HMS & SHMS

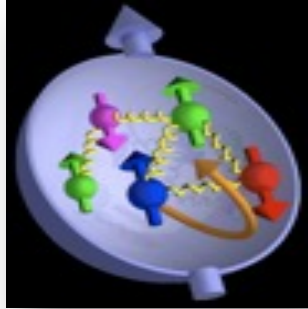


Hall-D: GlueX

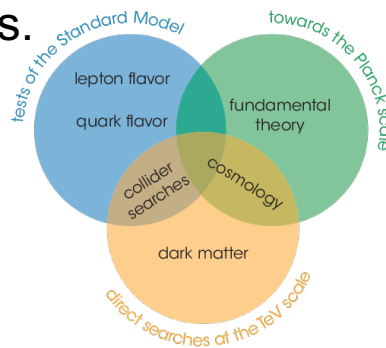


JLAB Physics program

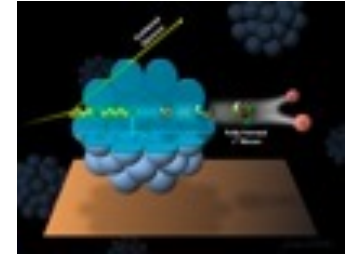
- Nucleon and nuclear structure studies, spatial and momentum tomography, form-factors ...



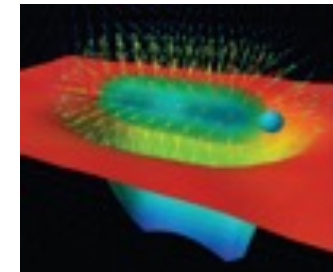
- Low-energy test of the Standard Model and fundamental symmetries, and search for Dark Matter particles.



- Cold nuclear matter, NN correlations, hadronization, color transparency...



- Exploring origin of confinement – meson and baryon spectroscopy, exotics ...

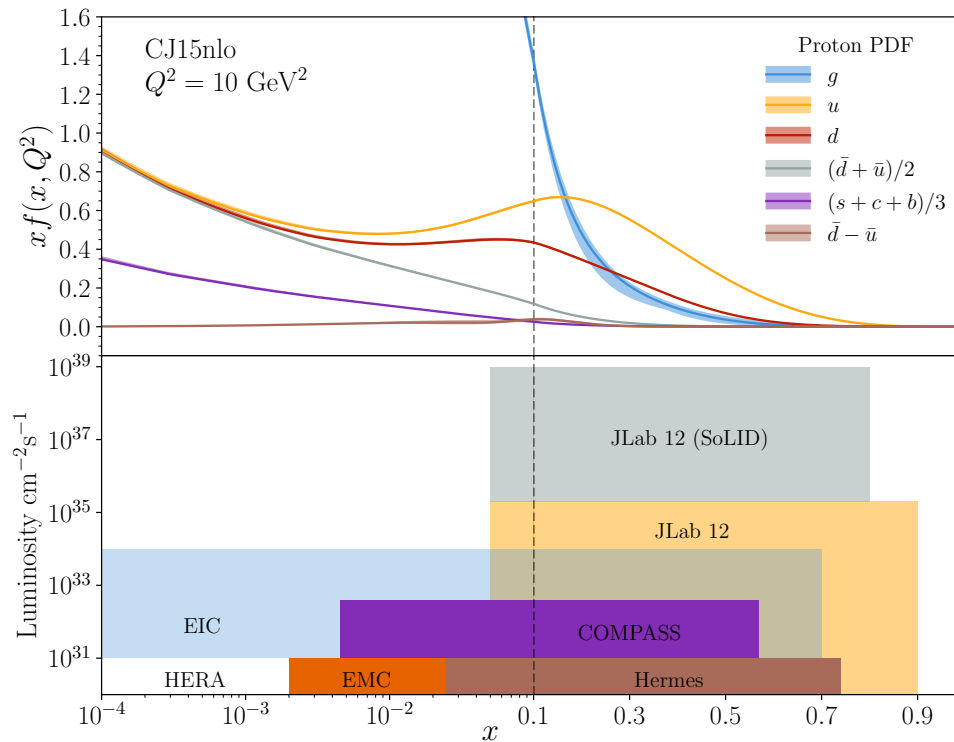


*Total of 91 approved experiments,
35 completed to date.*



Complementarity with facilities worldwide

Jefferson Lab stays very relevant and complementary to other facilities with the extremely high luminosity, high x reach of fixed target experiments.



- Precision measurements in the valence quark region requiring high luminosity are clearly the purview of CEBAF.
- The 20+ GeV energy upgrade will provide important overlap into the sea quark region where the EIC is designed to probe at low x .



Progress in Particle and Nuclear Physics
Volume 127, November 2022, 103985



Review

Physics with CEBAF at 12 GeV and future opportunities

J. Arrington^a, M. Battaglieri^{b, c}, A. Boehnlein^b, S.A. Bogacz^b, W.K. Brooks^j, E. Chudakov^b, I. Cloët^c, R. Ent^b, H. Gao^d, J. Grames^b, L. Harwood^b, X. Ji^{e, f}, C. Keppel^b, G. Krafft^b, R.D. McKeown^{b, h}, J. Napolitano^g, J.W. Qiu^{b, h}, P. Rossi^{b, n}, M. Schram^b, S. Stepanyan^b ... X. Zheng^k

Kinematic regions of Deep Inelastic Scattering and the comparative reach of different facilities.



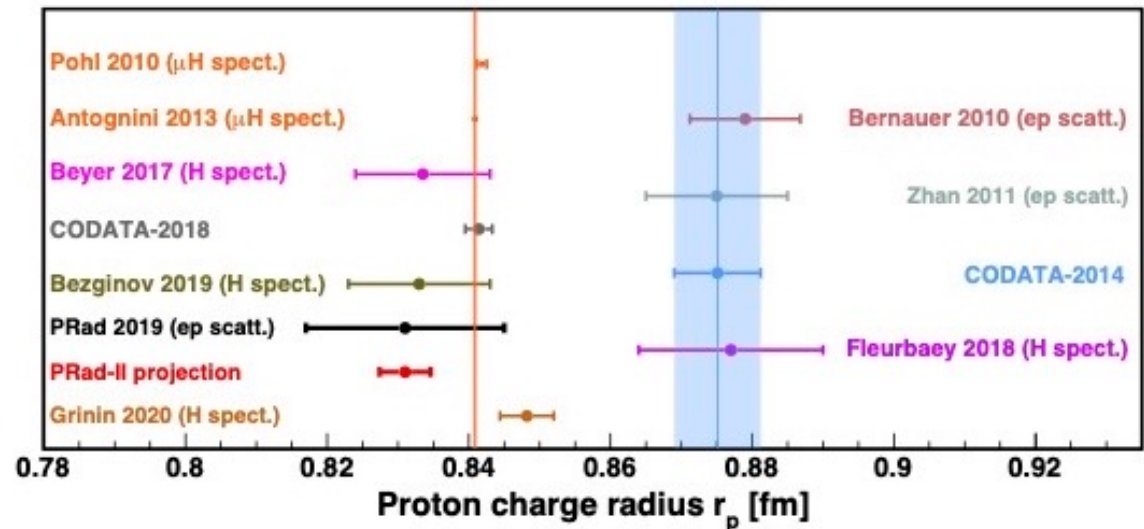
OFFICE OF
SCIENCE

S. Stepanyan, HEP2023, Jan. 9-13,
UTFSM, Valparaíso, Chile

Jefferson Lab
Thomas Jefferson National Accelerator Facility

EM form factors: proton radius puzzle

- Electron scattering has been a tool of choice for many decades for studies of the structure of the nucleon.
- At each new stage of experimental investigation, new challenges and inconsistencies arose. New experiments at Jefferson Lab address most of discrepancies, but some still remain.
- The “proton radius puzzle” – discrepancy between muonic-hydrogen and electron scattering – has been round for while.
- Proton radius experiment in Hall-B (PRad), was the first electron scattering experiment to reach Q^2 down to $2 \times 10^{-4} \text{ GeV}^2$ and obtained the proton radius $r_p = 0.831 \pm 0.007_{\text{stat}} \pm 0.012_{\text{syst}}$ fm, consistent with muonic-hydrogen data.

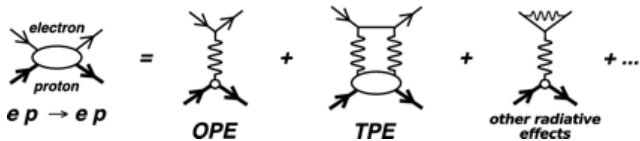


The approved PRad-II experiment will deliver the most precise measurement of G_E^p reaching the lowest ever Q^2 (10^{-5} GeV^2) in lepton scattering experiments, critical for the model-independent extraction of r_p .

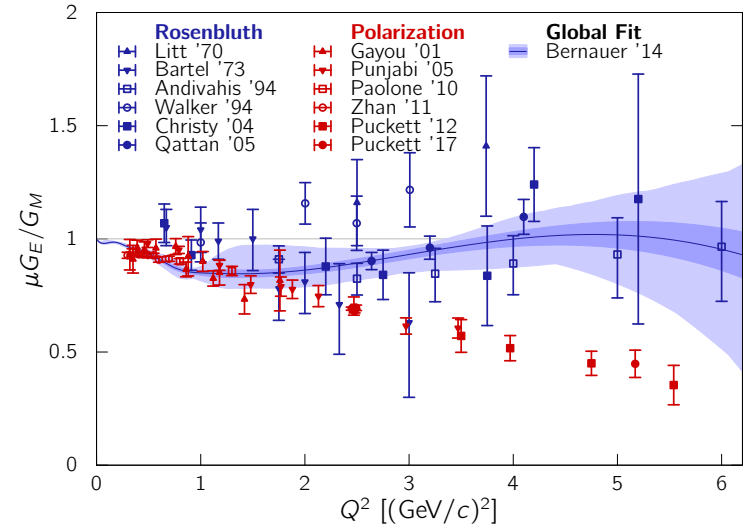


EM form factors: *high Q^2 behavior*

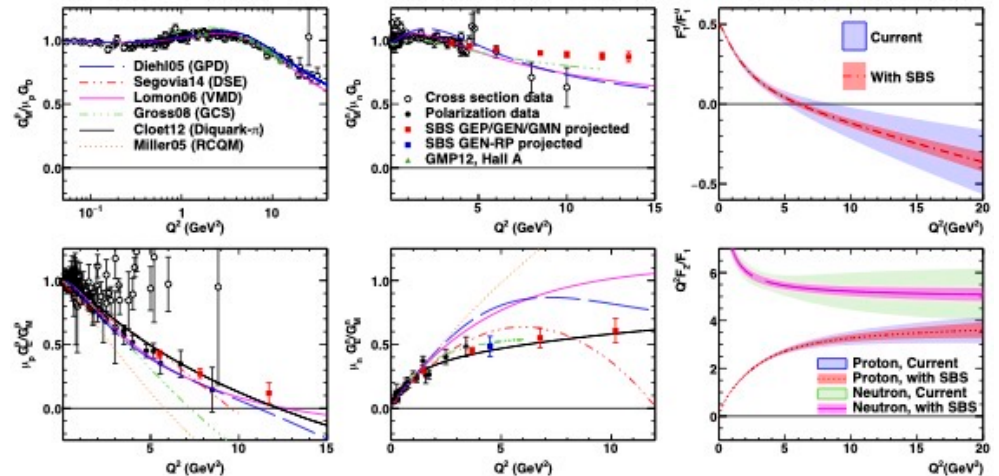
- Charge and magnetization distributions of nucleons has been characterized using elastic scattering down to very small impact parameter space (high Q^2), data dominated with experiments performed at Jefferson Lab.
- The high Q^2 behavior of the proton elastic form factors $G_E(Q^2)$ and $G_M(Q^2)$ has been a puzzle – discrepancy between measurements of high precision recoil polarization and the Rosenbluth separations – believe to be the result of higher order radiative corrections to the cross section, with a dominant two-photon exchange component.



- Experimental facilities at CEBAF will continue to tackle these questions, performing a new measurements with $Q^2 > 10 \text{ GeV}^2$.



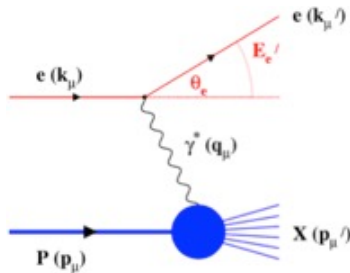
Projected FF results compared to existing data



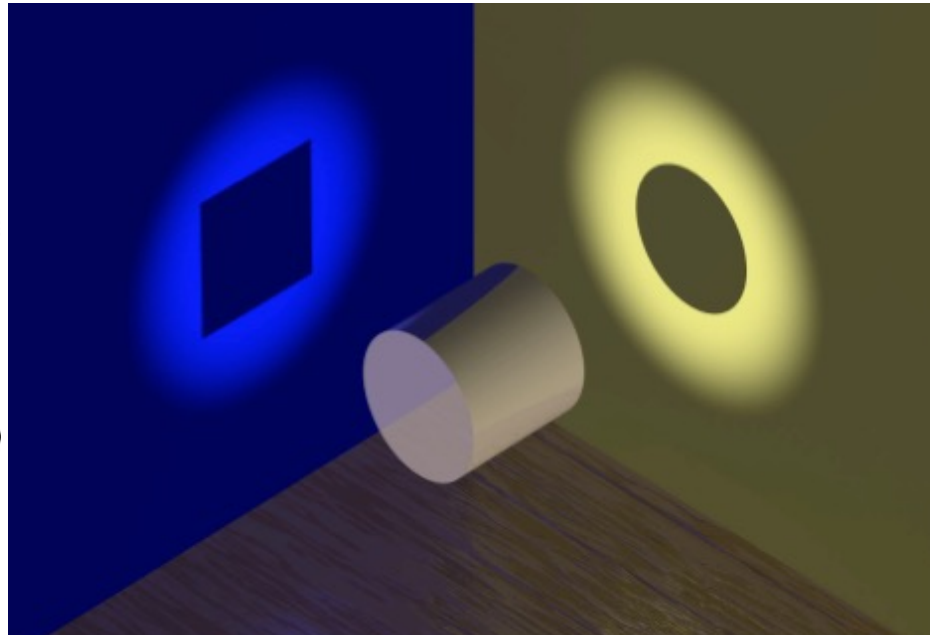
3-D Structure of the Nucleon

Elastic and deep inelastic scatterings give us two orthogonal projections.

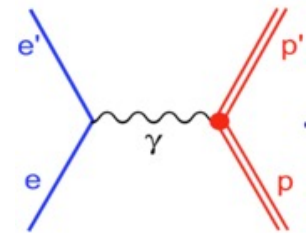
DIS Parton Distribution Functions



No information on the spatial location of the constituents



Elastic Form Factors



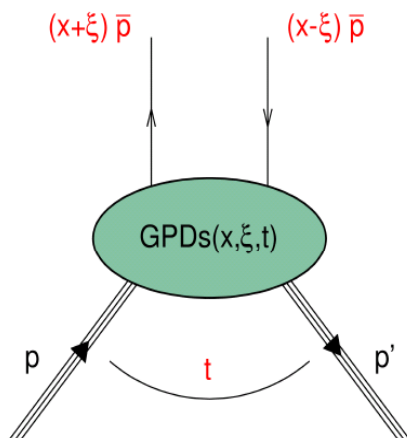
No information about the underlying dynamics of the system

Advances in theory over past 25 years – development of formalisms of **Generalized Parton Distributions** & Transverse Momentum Distributions – 3-D imaging of the nucleon's partonic structure, using deep exclusive and semi-inclusive reactions become a reality.



Nucleon tomography: GPD framework

- GPDs describe the correlation of quark/antiquark transverse spatial and longitudinal momentum, and the quark angular momentum distributions.
- GPDs are accessible through deep exclusive electron scattering reactions – a major thrust of the JLAB 12 GeV facility.



At leading-twist, there are four chiral-even (parton helicity-conserving) GPDs:

$$H^q; E^q; \tilde{H}^q; \tilde{E}^q$$

and four chiral-odd (parton helicity-flip) [Transversity] GPDs:

$$H_T^q, E_T^q, \tilde{H}_T^q, \tilde{E}_T^q$$

- **GPDs** → FFs (first moments of GPDs)

$$\int_{-1}^{+1} dx H^q(x, \xi, t) = F_1^q(t) \quad \int_{-1}^{+1} dx \tilde{H}^q(x, \xi, t) = g_A^q(t)$$

$$\int_{-1}^{+1} dx E^q(x, \xi, t) = F_2^q(t) \quad \int_{-1}^{+1} dx \tilde{E}^q(x, \xi, t) = h_A^q(t)$$

- **GPDs** → PDFs (in the limit $t \rightarrow 0$)

$$H^q(x, 0, 0) = q(x), -\bar{q}(-x)$$

$$\tilde{H}^q(x, 0, 0) = \Delta q(x), \Delta \bar{q}(-x)$$

- **T-GPDs** in the limit $t \rightarrow 0$:

Transversuty: $H_T^q(x, 0, 0) = h_1^q$

Tensor charge: $\int dx \tilde{H}_T(x, \xi, 0)$

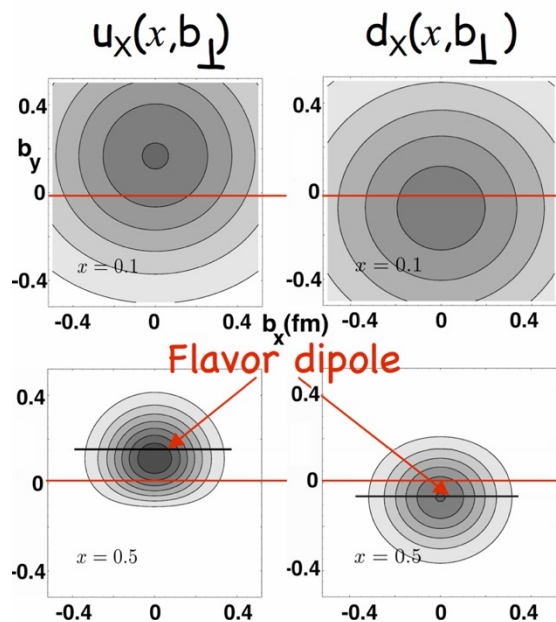
Anomalous tensor MM: $\kappa_T \int dx \tilde{E}_T(x, \xi, 0)$



Nucleon tomography and GFF from GPDs

Nucleon tomography

$$H^q(\mathbf{x}, \mathbf{b}_\perp) = \int \frac{d^2 \Delta_\perp}{(2\pi)^2} e^{-i\mathbf{b}_\perp \Delta_\perp} H^q(\mathbf{x}, \mathbf{0}, -\Delta_\perp^2)$$



M. Burkardt, Int.J.Mod.Phys.A18,2003

Decomposition of the nucleon spin

$$J_Q = \sum_q \frac{1}{2} \int_{-1}^1 dx \, x (H^q(\mathbf{x}, \xi, 0) + E^q(\mathbf{x}, \xi, 0))$$

Link to the energy-momentum tensor

$$\int_{-1}^1 dx \, x H^q(\mathbf{x}, \xi, t) = A^q(t) + \xi^2 D^q(t)$$

$$\int_{-1}^1 dx \, x E^q(\mathbf{x}, \xi, t) = B^q(t) - \xi^2 D^q(t)$$

Ji, Phys. Rev. Lett 77 / Phys. Rev. D 55, 1997.

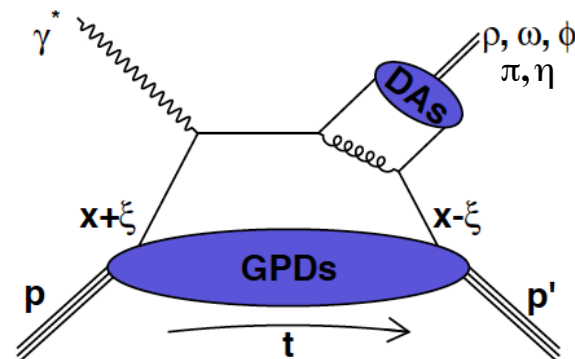
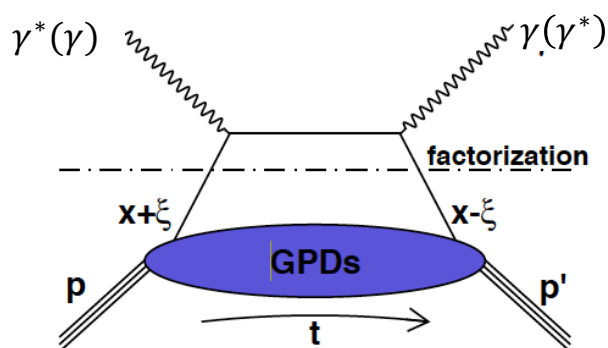
$$\text{Re}\mathcal{H}(\xi, t) = D(t) + \mathcal{P} \int_{-1}^1 dx \left(\frac{1}{\xi - 1} - \frac{1}{\xi + 1} \right) \text{Im}\mathcal{H}(\xi, t)$$

the D -term characterizes the distribution of forces inside the nucleon

Polyakov, Physics Letters B 555, 2003



Deep-exclusive reactions and GPDs



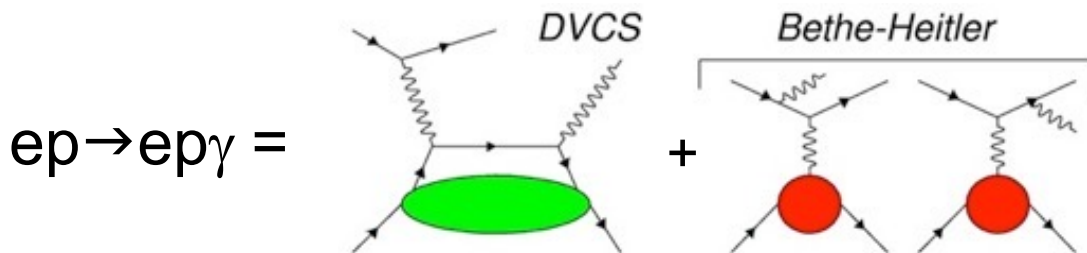
	Im (DVCS, TCS)	Re (DVCS, TCS)
\mathcal{H}	$A_{LU}, A_{\odot U}$	σ, A_{UU}
$\tilde{\mathcal{H}}$	A_{UL}	A_{LL}, A_{LT}
\mathcal{E}	A_{UT}	

A global analysis will be needed to fully disentangle GPDs

	Meson	Flavor
$\mathcal{H}_T, \mathcal{E}_T$	π^+	$\Delta u - \Delta d$
	π^0	$2\Delta u + \Delta d$
	η	$2\Delta u - \Delta d + 2\Delta s$
\mathcal{H}, \mathcal{E}	ρ^+	$u - d$
	ρ^0	$2u + d$
	ω	$2u - d$
	ϕ	g

DVCS – golden reaction for studying GPDs

Program covers measurements of beam helicity, longitudinal and transverse polarized target asymmetries using detectors in Halls A, B, and C.



$$\mathcal{T}^2 = |\mathcal{T}_{BH}|^2 + |\mathcal{T}_{DVCS}|^2 + \mathcal{T}_{DVCS}^* \mathcal{T}_{BH} + \mathcal{T}_{BH}^* \mathcal{T}_{DVCS}$$

$$\mathcal{T}_{DVCS} \sim CFF \quad \mathcal{H}(\xi, t) = \underbrace{i\pi [H(\xi, \xi, t) - H(-\xi, \xi, t)]}_{Im} + P \int_{-1}^{+1} dx \left(\frac{1}{\xi - x} \pm \frac{1}{\xi + x} \right) \underbrace{[H(x, \xi, t) \mp H(-x, \xi, t)]}_{Re}$$

Spin asymmetries, beam and target – p (n) and total cross sections,

$$A_{LU} \propto Im\tilde{\mathcal{H}} \quad A_{LL} \propto Re\tilde{\mathcal{H}}(\mathcal{H})$$

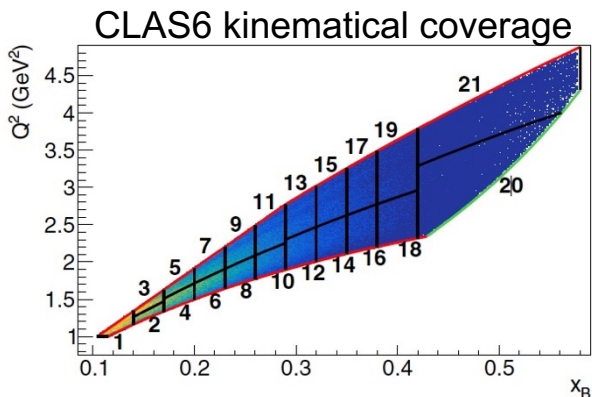
$$A_{UL} \propto Im\tilde{\mathcal{H}}(\mathcal{H}) \quad A_{UT} \propto Im\mathcal{E}(\mathcal{H})$$

and lepton charge asymmetries when positron beams will be available.



CLAS DVCS BSA and cross-sections

The first dedicated DVCS experiment with CLAS, 2005, uses a small angle calorimeter.

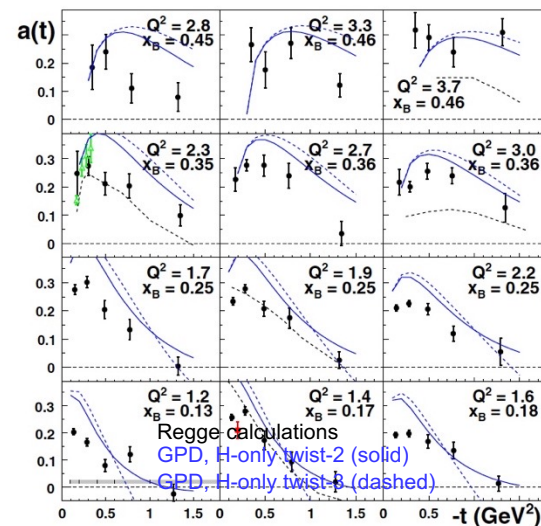


$$ep \rightarrow e'p'\gamma$$

The most extensive set of data at that time.

$$A_{LU} = \frac{a \sin \phi}{1 + c \cos \phi + d \cos 2\phi}$$

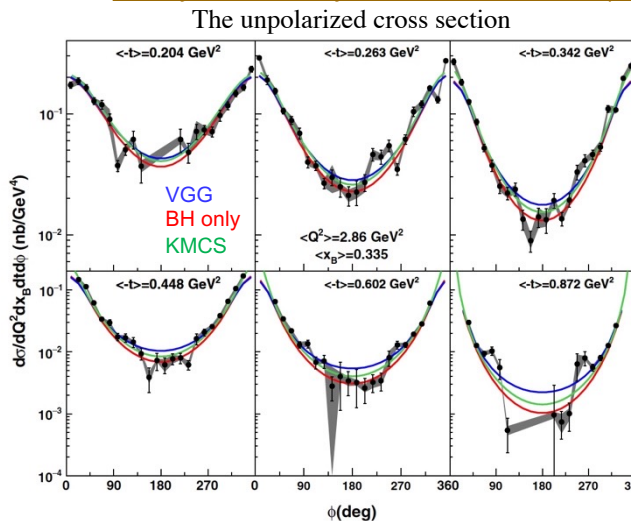
F.X. Girod et al., Phys. Rev. Lett **100**, 162002 (2008)



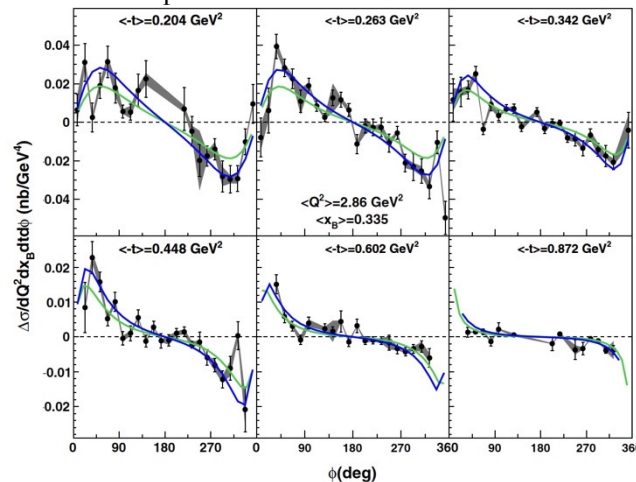
N. Saylor et al., Phys. Rev. C **98**, 045203 (2018)

Theoretical calculations from the Vanderhaeghen, Guichon, and Guidal (VGG) and Kroll, Moutarde, Sabatié, and Chouika (KMCS) models.

Both models generally reproduce the data, and the theory expectations are in fair agreement with the cross section and differences

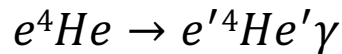


The polarized cross-section differences

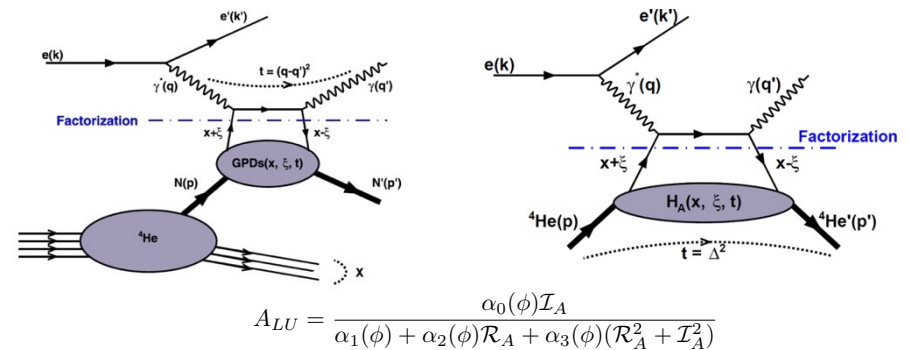
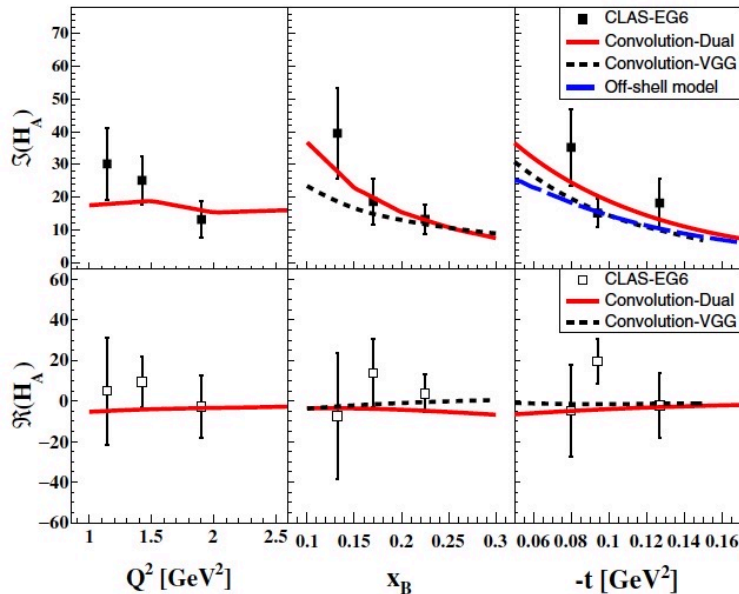


CLAS: Nuclear DVCS (^4He)

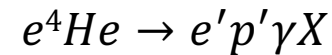
The first measurement of the beam-spin asymmetry in the fully exclusive process of coherent DVCS off a nucleus, $e^4\text{He} \rightarrow e'^4\text{He}'\gamma$, and incoherent off a bound proton, $e^4\text{He} \rightarrow e'p'\gamma X$.



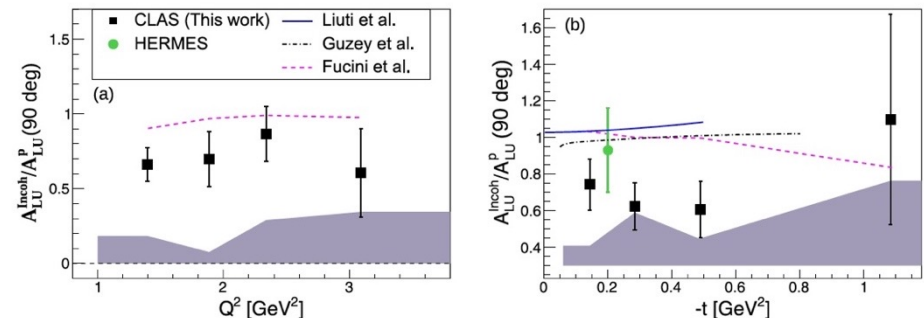
M. Hattawy et al., *Phys. Rev. Lett.* 119, 202004 (2017)



$$A_{LU} = \frac{\alpha_0(\phi)\mathcal{I}_A}{\alpha_1(\phi) + \alpha_2(\phi)\mathcal{R}_A + \alpha_3(\phi)(\mathcal{R}_A^2 + \mathcal{I}_A^2)}$$



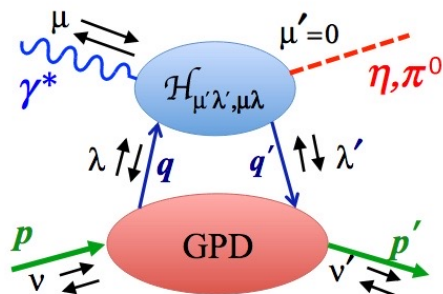
M. Hattawy et al., *Phys. Rev. Lett.* 123, 032502 (2019)



The ALERT program in Hall-B will take these studies to a whole new level using 11 GeV beams.



CLAS DVMP, π^0 and η



$$\frac{d^2\sigma}{dt d\phi_\pi} = \frac{1}{2\pi} \left[\left(\frac{d\sigma_T}{dt} + \epsilon \frac{d\sigma_L}{dt} \right) + \epsilon \cos 2\phi_\pi \frac{d\sigma_{TT}}{dt} + \sqrt{2\epsilon(1+\epsilon)} \cos \phi_\pi \frac{d\sigma_{LT}}{dt} \right].$$

The structure functions extracted from the fit to the ϕ distributions of the differential cross sections in kinematical bins of Q^2 , x_B , and t .

$$\frac{d\sigma_L}{dt} = \frac{4\pi\alpha}{k'} \frac{1}{Q^6} \left\{ (1 - \xi^2) |\langle \tilde{H} \rangle|^2 - 2\xi^2 \text{Re}[\langle \tilde{H} \rangle^* \langle \tilde{E} \rangle] - \frac{t'}{4m^2} \xi^2 |\langle \tilde{E} \rangle|^2 \right\}$$

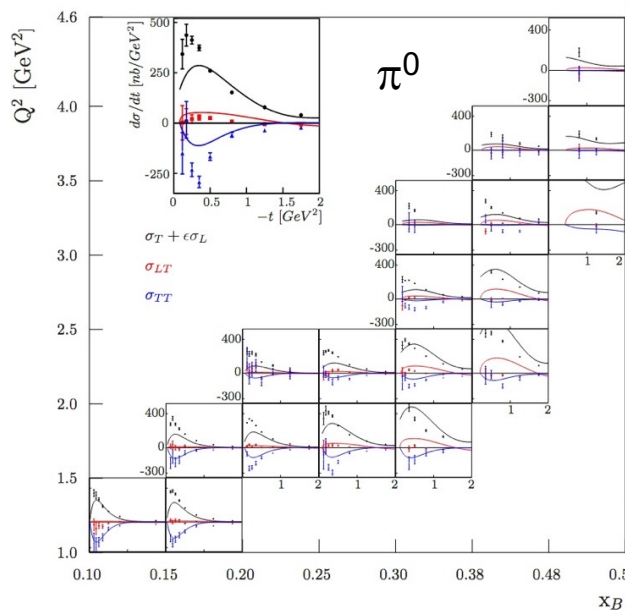
$$\frac{d\sigma_T}{dt} = \frac{4\pi\alpha}{2k'} \frac{\mu_\pi^2}{Q^8} \left[(1 - \xi^2) |\langle H_T \rangle|^2 - \frac{t'}{8m^2} |\langle \tilde{E}_T \rangle|^2 \right],$$

$$\frac{d\sigma_{LT}}{dt} = \frac{4\pi\alpha}{\sqrt{2}k'} \frac{\mu_\pi}{Q^7} \xi \sqrt{1 - \xi^2} \frac{\sqrt{-t'}}{2m} \text{Re}[\langle H_T \rangle^* \langle \tilde{E} \rangle],$$

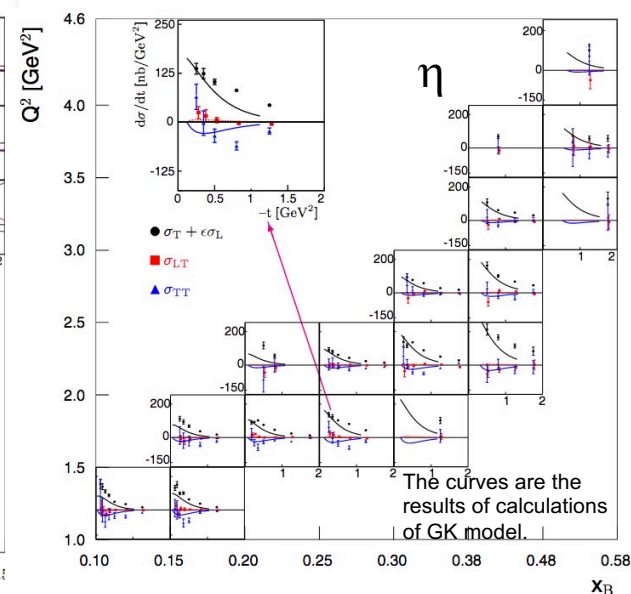
$$\frac{d\sigma_{TT}}{dt} = \frac{4\pi\alpha}{k'} \frac{\mu_\pi^2}{Q^8} \frac{t'}{16m^2} |\langle \tilde{E}_T \rangle|^2.$$

- For π^0 , $d\sigma_U/dt$ and $d\sigma_{TT}/dt$ are comparable in magnitude to each other while $d\sigma_{LT}/dt$ is quite small in comparison.
- In the handbag interpretation, Goloskovskov&Kroll (GK), data hint to a large contribution of \tilde{E}_T .
- The cross-section ratios of η to π^0 appear to agree with the handbag calculations at low $|t|$ but show significant deviations with increasing $|t|$.

I. Bedlinskiy et al., PRC **90**, 025205 (2014)



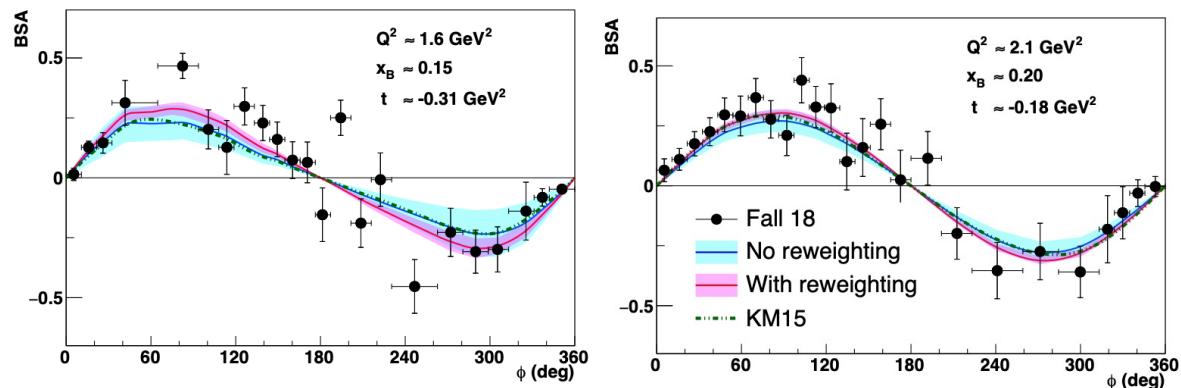
I. Bedlinskiy et al., PRC **95**, 035202 (2017)



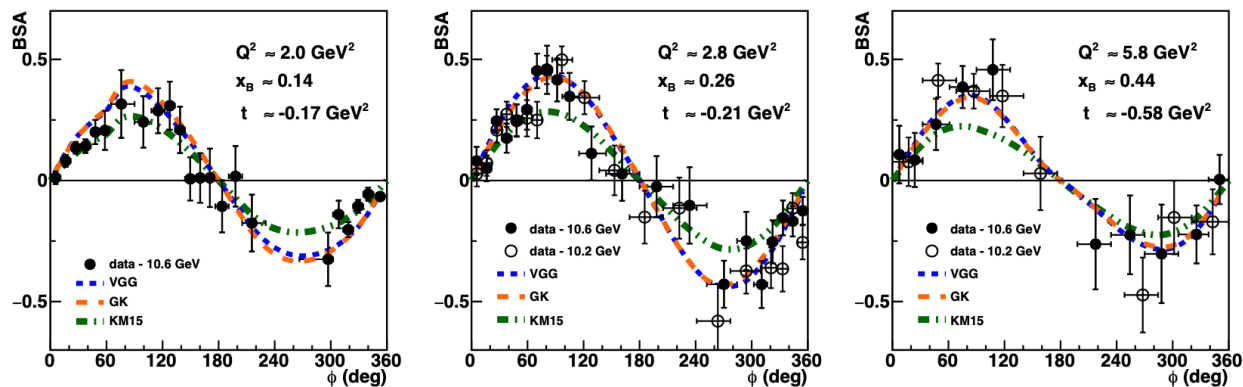
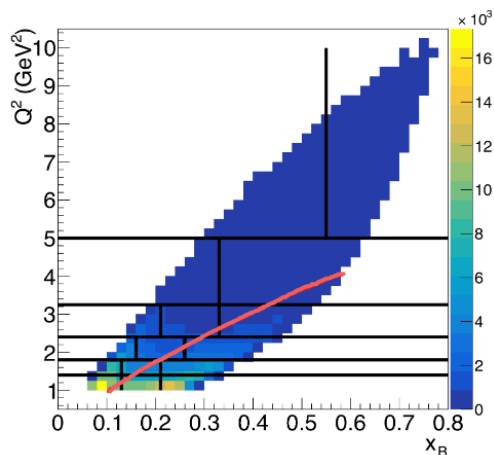
DVCS – BSA with CLAS12

$$A_{LU} = \frac{a \sin \phi}{1 + c \cos \phi + d \cos 2\phi}$$

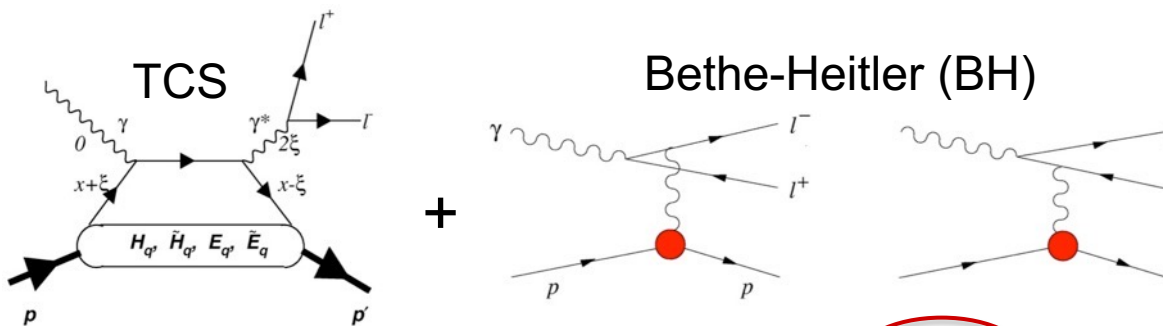
Fit with PARTONS ANNs, constrained on 6 GeV data.



Comparisons with KM15 and VGG/GK models.



First measurements of TCS with CLAS12

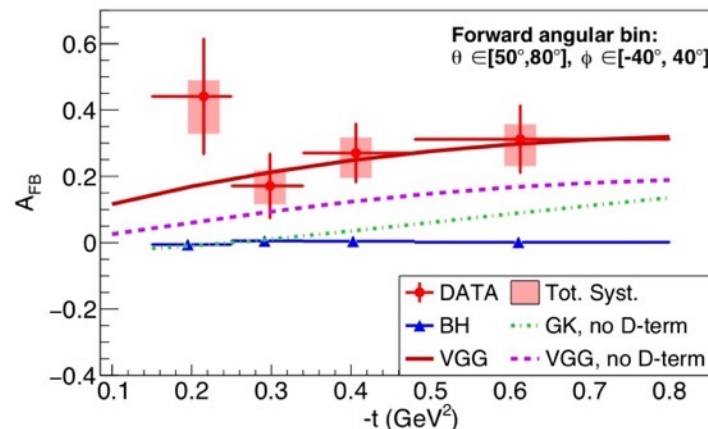
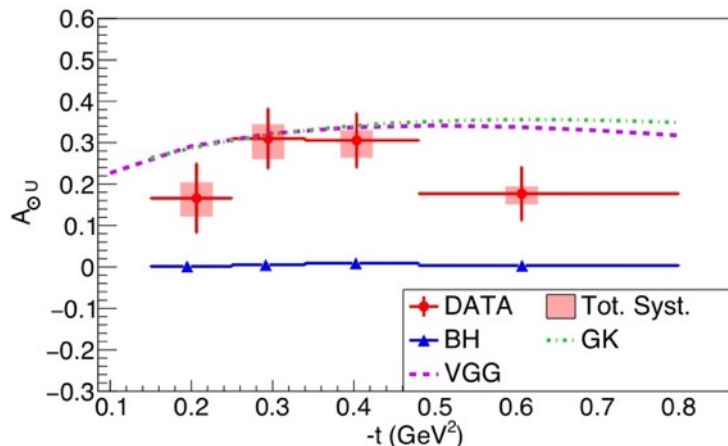


$$\sigma(\gamma p \rightarrow p' e^+ e^-) = \sigma_{\text{BH}} + \sigma_{\text{TCS}} + \sigma_{\text{INT}}$$

- BHA, $A_{\text{OU}} \sim \sin \phi \text{Im} \tilde{M}^{--}$, universality of GPDs
- FB asymmetry, $A_{\text{FB}} \sim \cos \phi \text{Re} \tilde{M}^{--}$, access to the EM FF $D^q(t)$ (D-term).

$$A_{\text{OU}} = \frac{1}{P_b} \frac{N^+ - N^-}{N^+ + N^-} = \frac{d\sigma^+ - d\sigma^-}{d\sigma^+ + d\sigma^-} = \frac{-\frac{\alpha_{\text{em}}^3}{4\pi s^2} \frac{1}{-t} \frac{m_p}{Q'} \frac{1}{\tau\sqrt{1-\tau}} \frac{L_0}{L} \sin \phi \frac{(1+\cos^2 \theta)}{\sin(\theta)} \text{Im} \tilde{M}^{--}}{d\sigma_{\text{BH}}}$$

$$A_{\text{FB}}(\theta_0, \phi_0) = \frac{d\sigma(\theta_0, \phi_0) - d\sigma(\pi - \theta_0, \pi + \phi_0)}{d\sigma(\theta_0, \phi_0) + d\sigma(\pi - \theta_0, \pi + \phi_0)} = \frac{-\frac{\alpha_{\text{em}}^3}{4\pi s^2} \frac{1}{-t} \frac{m_p}{Q'} \frac{1}{\tau\sqrt{1-\tau}} \frac{L_0}{L} \cos \phi_0 \frac{(1+\cos^2 \theta_0)}{\sin(\theta_0)} \text{Re} \tilde{M}^{--}}{d\sigma_{\text{BH}}(\theta_0, \phi_0) + d\sigma_{\text{BH}}(\pi - \theta_0, \pi + \phi_0)}$$



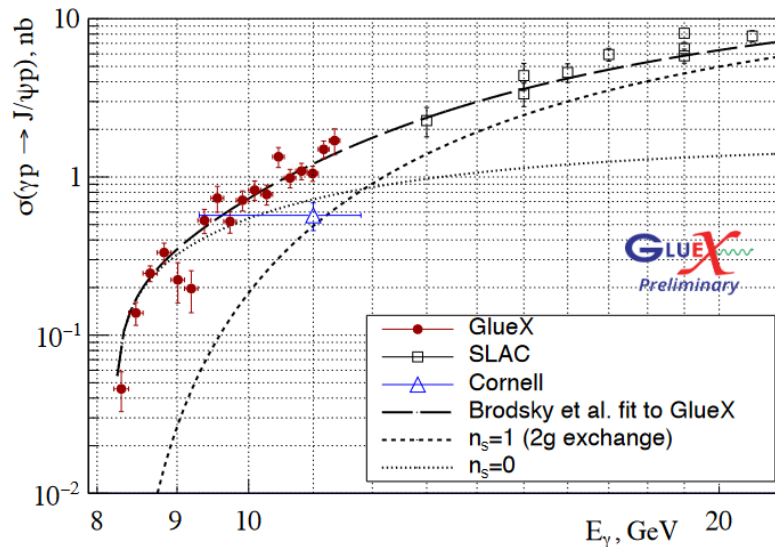
P. Chatagnon, et al. (CLAS Collaboration), "Phys. Rev. Lett. 127, 262501 (2021).



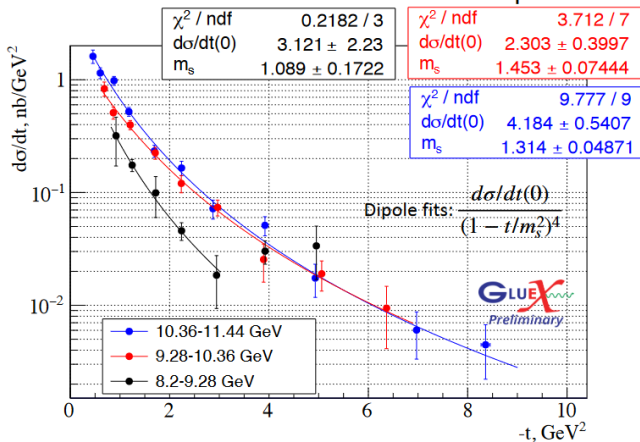
Protons gluonic FF – near threshold J/ψ production

- Directly probe nucleon's gluonic field, access to the matter distribution, mass radius, and the trace anomaly of the EMT.
- Experiments in Hall C, and D (GlueX) already published results, the Hall-B CLAS12 (p, n) will follow.

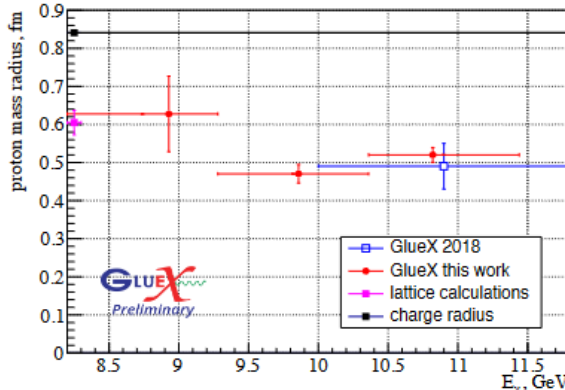
Total cross section asymptotic - power counting



Differential cross-sections - forward extrapolation



E_γ, GeV	8.93	9.86	10.82
$q_{c.m.}, \text{GeV} (J/\psi \text{ c.m.})$	0.499	0.767	0.978
$d\sigma/dt(0), \text{nb}/\text{GeV}^2$	3.121 ± 2.23	2.303 ± 0.400	4.184 ± 0.541
m_s, GeV	1.089 ± 0.172	1.453 ± 0.074	1.314 ± 0.049



$$r_m = \frac{6}{m_p} \frac{dG}{dt} \Big|_{t=0} = \frac{12}{m_s^2}$$

D.Kharzeev PRD104(2021)



A need for a large acceptance facility with $L \geq 10^{37} \text{ cm}^{-2} \text{ sec}^{-1}$

First experimental measurement with CLAS12 PRL 127, 262501 (2021)

Started in 2001, PRL 87, 182002. Now is the flagship physics program

JLAB Flagship program – accessing GPDs through measurements of beam/target asymmetries and the cross sections of Compton processes (TCS and DVCS)

TCS

Hard scale is defined by time-like photons

Access to the Re-part of the Compton amplitude

$$\text{Re } \mathcal{H}(\xi, t) = PV \int_{-1}^1 dx C^-(\xi, x) H(x, \xi, t)$$

$$\text{Im } \mathcal{H}(\xi, t) = i\pi H(\xi, \xi, t)$$

DVCS

Hard scale is defined by space-like photon

Jefferson Lab at the luminosity frontier is the only place in the world DDVCS can be measured!

μ CLAS12 in Hall B and SoLID in Hall A are the two proposed facilities capable of carrying out such measurements.

DDVCS

Both space-like and time-like photons can set the hard scale

$$\int_{-1}^{+1} dx \frac{H(x, \xi, t)}{x - (2\xi' - \xi) + i\epsilon} + \dots$$

$$H(2\xi' - \xi, \xi, t) + H(-(2\xi' - \xi), \xi, t)$$

σ -DDVCS is three orders of magnitude smaller than σ -DVCS



GPDs in Virtual Compton Scattering

Space-like Photon

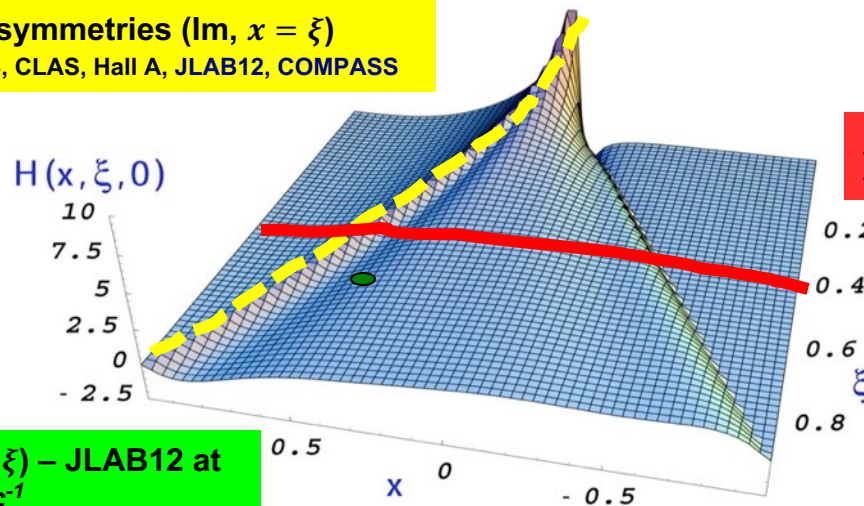
$ep \rightarrow ep$

$$\mathcal{T}^2 = |\mathcal{T}_{BH}|^2 + |\mathcal{T}_{DVCS}|^2 + \mathcal{T}_{DVCS}^* \mathcal{T}_{BH} + \mathcal{T}_{BH}^* \mathcal{T}_{DVCS}$$

$$\gamma \overline{\mathcal{T}}_{DVCS} \sim CFF \mathcal{H}(\xi, t) = i\pi \underbrace{[H(\xi, \xi, t) - H(-\xi, \xi, t)]}_{Im} + P \int_{-1}^{+1} dx \underbrace{\left(\frac{1}{\xi - x} \pm \frac{1}{\xi + x} \right) [H(x, \xi, t) \mp H(-x, \xi, t)]}_{Re}$$

Spin asymmetries ($Im, x = \xi$)

HERMES, CLAS, Hall A, JLAB12, COMPASS



Angular asymmetry in TCS ($|Re|$)
JLAB12

Charge asymmetry in DVCS ($|Re|$)
HERMES, COMPASS, JLAB12

DVCS Cross sections ($|Re|^2$)
H1, Hall A, JLAB12, COMPASS

DDVCS ($Im, x \neq \xi$) – JLAB12 at
 $L \geq 10^{37} \text{ cm}^{-2} \text{ sec}^{-1}$

Re parts of CFFs provides a direct measurement of the D-term and access to the mechanical properties of the proton



OFFICE OF
SCIENCE

S. Stepanyan, HEP2023, Jan. 9-13,
UTFSM, Valparaíso, Chile

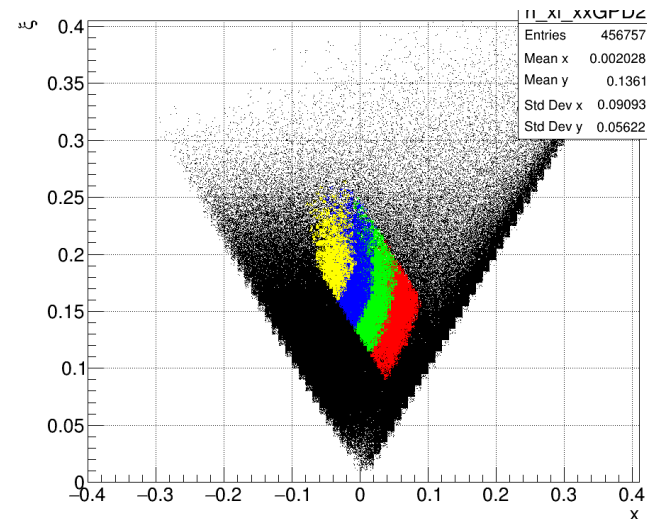
Jefferson Lab
Thomas Jefferson National Accelerator Facility

High luminosity facilities for DDVCS

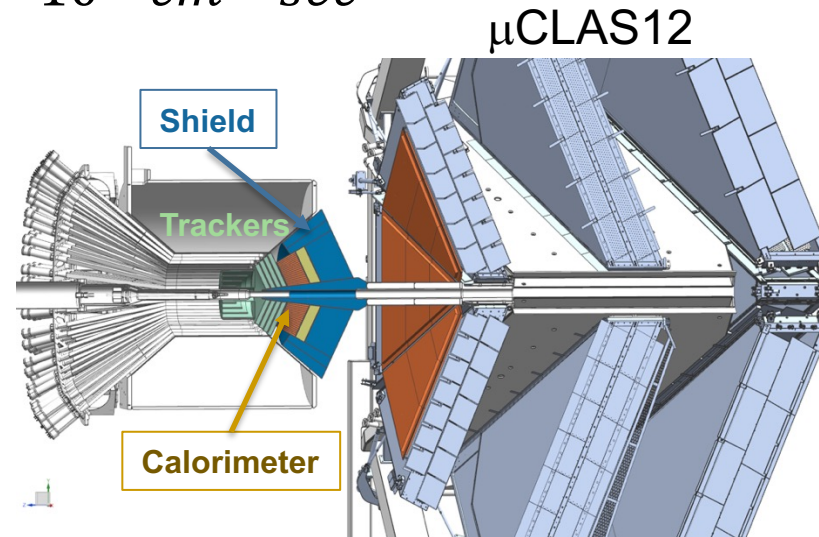
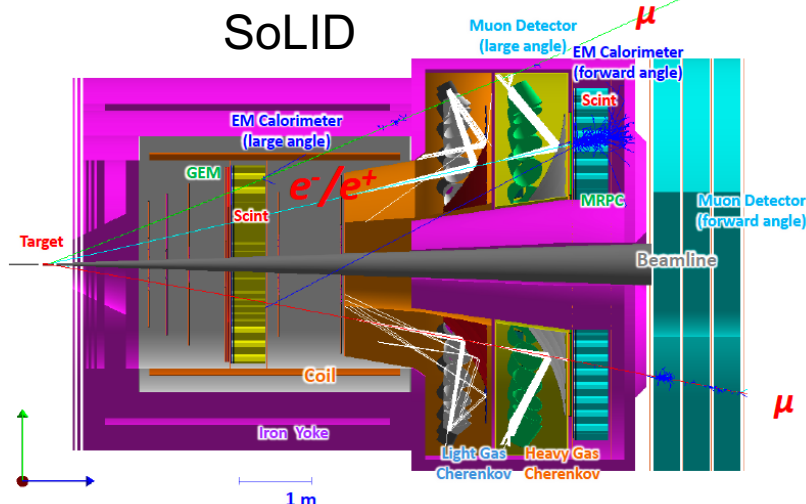
Challenges in DDVCS measurements:

- Cross section is two to three orders of magnitude smaller than the DVCS cross section;
- Ambiguities and anti-symmetrization issues with the decay leptons of the outgoing virtual photon and the incoming-scattered lepton.

Both challenges can be solved by studying di-muon electroproduction.



$$ep \rightarrow e' p' \mu^+ \mu^- @L > 10^{37} \text{ cm}^{-2} \text{ sec}^{-1}$$



Summary

- Jefferson lab is home to high luminosity experiments and will remain the prime facility for fixed target electron scattering for decades to come.
- The execution of a vibrant physics program with up to 12 GeV electron beams is ongoing and will continue for the next 15 years or more.
- New experiments yielded ground-breaking Nuclear Physics results in -
 - 3-D imaging of the nucleon, spatial and momentum tomography
 - isospin decomposition of nucleon structure functions,
 - near-threshold J/ψ production, proton mass decomposition, gluonic FFs
 - proton charge radius measurement, and
 - new information on neutron matter.
- There are exciting physics opportunities with positron beams, and proposals are coming to JLAB PAC.
- Looking forward to a new round of upgrades, building a case for high energy, >20 GeV, machine.

